Thermal Resistance Models of Packed-Bed Effective Heat Transfer Parameters

Simple thermal resistance models of packed-bed heat transfer can be used to derive predictive formulas for the effective axial and radial thermal conductivities and apparent wall heat transfer coefficient. In particular, the behavior of the heat transfer parameters over the entire range of Reynolds number can be explained by considering the two asymptotic cases of low *Re* (solid phase dominant) and high *Re* (fluid phase dominant).

A. G. DIXON

Department of Chemical Engineering
Worcester Polytechnic Institute
Worcester, MA 01609

SCOPE

The modeling of heat transfer in packed beds is a topic of great importance in the analysis and design of catalytic reactors. A packed bed is an extremely complex random geometrical arrangement, and any tractable model must represent a greatly simplified description. In particular, pseudo-homogeneous models have enjoyed widespread acceptance, due to their convenient mathematical form. The many heat transfer phenomena of a packed bed are lumped into only a few effective parameters in such models, making it very difficult to extrapolate empirical correlations from laboratory conditions up to plant-size equipment, as the controlling heat transfer mechanisms may be quite different.

The simplest representation of radial heat transfer uses a single overall heat transfer coefficient U in a one-dimensional model of axial temperature profiles. Wellauer et al (1982) have shown that this quantity must be carefully built up from the effective radial conductivity k_r and apparent wall heat transfer coefficient h_w of a two-dimensional model, rather than relying on empirical correlations. The k_r and h_w must in turn be predicted from correlations for the individual fluid and solid phase parameters, which represent few enough physical phenomena to be safely extrapolated.

A set of parameter relations for steady state heat transfer has been presented by Dixon and Cresswell (1979), which successfully predicted limited data on k_r and h_w from the underlying two-phase model parameters. The derivation of the formulas and the formulas themselves involved much mathematical manipulation, put a special emphasis on the fluid phase, and did not appear to admit to a physical interpretation. The testing of the formulas was also limited by the lack of reliable correlations for the individual fluid and solid contributions.

Recent results of radial fluid dispersion of heat and mass (Dixon et al., 1984) and solid conduction (Melanson and Dixon, 1985) have remedied this situation and have suggested a greater influence of the solid phase, especially at low tube-to-particle diameter ratios, than had at first been supposed. Some systematic deviation of the predicted h_w from experimental data was also observed.

The objective of this study is to generalize, extend, and provide a physical interpretation of the parameter relations found previously. This is done by showing that previous formulas correspond to certain thermal resistance models of fixed-bed heat transfer. This interpretation provides an intuitive method of deriving alternative parameter relations, simply by choosing different resistance networks, which may include the original models as special cases. Likely candidates can usually be justified by mathematical analysis and compare favorably with reliable experimental data.

CONCLUSIONS AND SIGNIFICANCE

The overall heat transfer coefficient based on the bed average temperature is given by

$$\frac{1}{U} = \frac{1}{h_w} + \frac{R}{4k_r}$$

which relates one- and two-dimensional fixed-bed heat transfer models.

The formulas relating one- and two-phase models are

1. Effective axial conductivity

$$k_a = k_{af} + k_{as}$$

2. Effective radial conductivity and apparent wall heat transfer coefficient

$$k_r \frac{Bi}{Bi+4} = k_{rf} \frac{Bi_f}{Bi_f+4} + k_{rs} \frac{Bi_s}{Bi_s+4}$$

$$Bi \equiv \frac{h_w R}{k_r} = \begin{cases} Bi_f (\equiv h_{wf} R/k_{rf}) & \text{(high } Re\text{)} \\ Bi_s (\equiv h_{ws} R/k_{rs}) & \text{(low } Re\text{)} \end{cases}$$

Comparison with experiment shows that good prediction of k_r is obtained using the high Re version ($Bi = Bi_f$) for $Re > 50$, which covers the practical range of reactor operation. For Bi itself, good estimates may be obtained from $Bi = Bi_f$ for $Re > 1000$, and from $Bi = Bi_s$ for $Re < 10$. These will usually overestimate Bi; the formula

$$\frac{1}{Bi} = \frac{1}{Bi_f} + \frac{1}{Bi_s}$$

appears to underestimate Bi and is often more accurate in the intermediate range.

These formulas have a simple physical interpretation in terms of thermal resistances and can be verified by mathematical analysis. They include only those terms of importance in steady state model matching. For the transient case, completely different formulas may be necessary, as shown for k_a by Cresswell and Dixon (1982).

Correlations for individual phase parameters for low d_t/d_p and various packing shapes are fast becoming available, so that

use of these parameter relations should allow a range of sophistication in steady state fixed-bed heat transfer modeling over the entire range of Reynolds number, particle conductivity, particle size and shape, and equipment dimensions.

INTRODUCTION

The main heat transport processes in a fixed bed may be represented by individual phase thermal conductivities and by heat transfer coefficients, as shown in Figure 1 for the case of spheres as packing. The bed is essentialiy divided into a mixing phase (flowing fluid) and a conduction phase (solid plus stagnant fluid). All radial transport through the mixing phase is lumped into k_{rf} and through the conduction phase into k_{rs}. All axial transport, apart from bulk flow at the bed superficial mass flow rate G, is similarly lumped into k_{af} and k_{as}. Interphase heat transfer is included in the coefficient h, which also contains the resistance to solid conduction from the surface of a pellet to that point where the average pellet temperature is attained. Additional resistances are placed at the wall in each phase, reflecting a decrease in k_{rs} near the wall, due to the higher void fraction resulting from the change in packing geometry, and also a decrease in k_{rf}, due to the damping of turbulent eddies near the wall. These are represented by the transfer coefficients h_{ws} and h_{wf}, respectively.

Fixed beds are commonly modeled by pseudo-continuum models; these may be one- or two-dimensional, depending on whether radial temperature profiles are important, and may explicitly include both phases or only a single pseudo-homogeneous phase. The transport processes enter into single-phase two-dimensional models by way of effective bed conductivities k_a and k_r and an apparent wall heat transfer coefficient h_w. A one-dimensional model lumps all radial resistance into a single overall heat transfer coefficient U, as discussed in the following section.

As the level of complexity of the models decreases, the number of heat transfer parameters needed in each model also decreases; however, those parameters must make up for this by representing more and more heat transfer phenomena. It therefore becomes very difficult to obtain empirical correlations for such parameters and very dangerous to extrapolate such correlations from lab conditions to the equipment sizes and flow rates of industrial practice. One way of circumventing this difficulty is to provide relationships between the more fundamental two-phase model parameters, which presumably may be more readily correlated and extrapolated, and the effective parameters of simpler models. The designer of fixed beds is thereby provided with a hierarchy of models from which to choose and the means to quickly and reliably convert from one to another.

Formulas relating the one- and two-phase two-dimensional model parameters have been presented by Dixon and Cresswell (1979) and were later used by Wellauer et al. (1982) to obtain overall heat transfer coefficients. These formulas were obtained by a perturbation-collocation analysis of the model equations, and a subsequent matching of the one-phase and fluid phase temperature profiles. It is desirable to remove the asymmetry of treatment by considering also the solid phase, and also to understand the parameter relations in terms of their physical implications for fixed-bed heat transfer. This is attempted in this work by the use of thermal resistance models.

Any resistance model of such a complex geometrical configuration as a packed bed must represent a greatly simplified picture if it is to be of any use for quantitative prediction. The purpose here is to present models of limiting cases, which may be used to extend and generalize the previous model-matching formulas of Dixon and Cresswell (1979), which will be shown to correspond to the limiting case of relevance to fixed-bed reactor design, namely, the high flow rate asymptote.

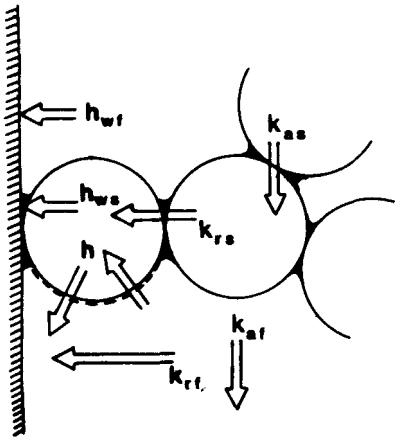

Figure 1. Fixed-bed heat transfer mechanisms and parameters.

RELATIONS BETWEEN ONE- AND TWO-DIMENSIONAL MODELS

It is preferable to use one-dimensional fixed-bed models whenever possible, as ordinary, rather than partial, differential equations result. This is especially necessary in studies of reactor control. In such models the radial heat transfer is represented by a single parameter

$$\begin{aligned} &\text{a) } q_r^{(1)} = U(T_{av} - T_w) \\ &\text{b) } q_r^{(1)} = U'(T_c - T_w) \\ &\text{c) } q_r^{(1)} = -\bar{k}_r \left.\frac{\partial T}{\partial r}\right|_{r=R} \end{aligned} \tag{1}$$

Wellauer et al. (1982) have shown that the overall heat transfer coefficient U' must be carefully built up from k_r and h_w, where

$$\left. q_r^{(2)} \right|_{r=R} = -k_r \left.\frac{\partial T}{\partial r}\right|_{r=R} = h_w (T - T_w)\Big|_{r=R} \tag{2}$$

and these in turn from the two-phase parameters, to get good prediction of the temperature profile in low d_t/d_p beds.

Relations between the parameters have been reviewed by Hlavacek (1970) and Froment (1972). An addition of resistances formula can be found by one-point collocation (Finlayson, 1971; Villadsen and Michelsen, 1978) or other methods:

$$\frac{1}{U} = \frac{1}{h_w} + \frac{R}{\alpha k_r} \tag{3}$$

Various values of α have been used, corresponding essentially to different choices of collocation point. Beek and Singer (1951) found $\alpha = 4$ in an early study, while more recently Crider and Foss (1965) obtained $\alpha = 6.133$ and Finlayson (1971) recommends $\alpha = 3$. For finite Bi, Villadsen and Michelsen (1978) show that the best choice is that which leads to $\alpha = 4$.

Wellauer et al. (1982) used asymptotic flux matching (i.e., they used the first term only of the infinite series solution to the model equations) to obtain

$$U' = h_w J_o(\lambda_1) \tag{4a}$$

where λ_1 is the smallest root of $BiJ_o(\lambda) - \lambda J_1(\lambda) = 0$. If λ_1 is approximated by $\lambda_1 = 8Bi/(Bi + 4)$, and also $J_o(\lambda_1) \simeq 1 - \lambda_1^2/4$, both of which are good for small Bi, then

$$\frac{1}{U'} = \frac{1}{h_w} + \frac{2R}{k_r}\frac{1}{4 - Bi} \to \frac{1}{h_w} + \frac{R}{2k_r} \tag{4b}$$

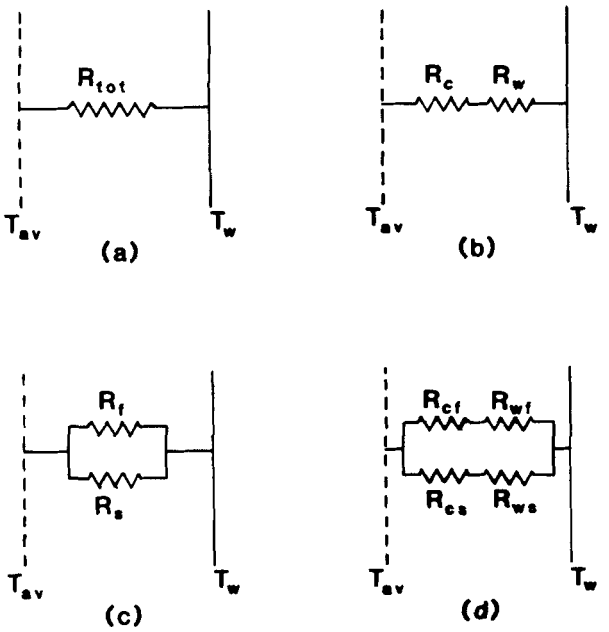

Figure 2. Resistance models of fixed-bed heat transfer.

as $Bi \to 0$, which has previously been given by Froment (1972).

In the present work, a relation is needed for $\bar{k}_r$, and this is readily derived as

$$\frac{R}{4\bar{k}_r} = \frac{1}{h_w} + \frac{R}{4k_r} \tag{5}$$

or in dimensionless form, introducing fluid molecular conductivity k_f, as

$$\frac{\bar{k}_r}{k_f} = \frac{k_r}{k_f}\frac{Bi}{Bi + 4} \tag{6}$$

Similar relations may be derived between the one-dimensional and two-dimensional two-phase models, giving

$$\frac{\bar{k}_{rs}}{k_f} = \frac{k_{rs}}{k_f}\frac{Bi_s}{Bi_s + 4} \tag{7a}$$

$$\frac{\bar{k}_{rf}}{k_f} = \frac{k_{rf}}{k_f}\frac{Bi_f}{Bi_f + 4} \tag{7b}$$

THERMAL RESISTANCE MODELS OF RADIAL HEAT TRANSFER

A pseudo-homogeneous fixed-bed heat transfer model may represent the radial resistance as either a single resistance for the whole bed (Figure 2a) or as bed center and near-wall resistances in series (Figure 2b).

In this work, all resistances will be based on unit wall area, so that the area terms may be omitted for clarity. The total bed resistance (with respect to the temperature difference $(T_{av} - T_w)$) may be interpreted as

$$R_{tot} = \frac{1}{U} = \frac{R}{4\bar{k}_r} \tag{8}$$

or as

$$R_{tot} = R_c + R_w = \frac{R}{4k_r} + \frac{1}{h_w} \tag{9}$$

which follows directly from Eq. 5.

A pseudo-continuum two-phase model might well be represented as shown in Figures 2c and 2d, in which case similar resistance formulas hold:

$$R_f = \frac{R}{4\bar{k}_{rf}} \tag{10}$$

$$R_f = R_{cf} + R_{wf} = \frac{R}{4k_{rf}} + \frac{1}{h_{wf}} \tag{11}$$

$$R_s = \frac{R}{4\bar{k}_{rs}} \tag{12}$$

$$R_s = R_{cs} + R_{ws} = \frac{R}{4k_{rs}} + \frac{1}{h_{ws}} \tag{13}$$

and

$$\frac{1}{R_{tot}} = \frac{1}{R_f} + \frac{1}{R_s} \tag{14}$$

The interphase resistance, R_{fs}, presents problems both in its location in the network and in the solution of the resulting network. Previous work (Cresswell and Dixon, 1982; Melanson and Dixon, 1985) suggests that this term is of lesser importance in steady state modeling, and it will be modified in the following exposition for mathematical convenience. The expression of R_{fs} in terms of h now completes the catalogue. The solid-to-fluid resistance is represented by the lumped parameter h where

$$\frac{1}{h} = \frac{1}{h_{fs}} + \frac{R_p}{(s + 3)k_p} \tag{15}$$

and h is defined with respect to the difference between the fluid temperature and the average solid particle temperature for the continuum model.

Here h is based on unit particle surface area and must be corrected to the same basis as the other transfer resistances. The conversion is made by

$$h(\text{surface area of packing})$$
$$= h(\text{surface area of wall})\left(\frac{\text{surface area of packing}}{\text{packing volume}}\right)\left(\frac{\text{packing volume}}{\text{surface area of wall}}\right)$$
$$= ha\frac{R}{2}(\text{surface area of wall}).$$

Thus $haR/2$ is the interphase transfer coefficient based on unit wall surface area, showing that

$$R_{fs} = \frac{2}{haR} \tag{16}$$

The various resistances have now all been expressed in terms of transport parameters, and thermal resistance models may be proposed to give relations between the parameters.

High *Re* Case

For high flow rates the main transport mechanism is by turbulent mixing in the fluid phase. When this is much faster than solid phase conduction, most of the energy is transferred directly through the fluid phase and does not pass through the interphase resistance. Thus the simplified picture shown in Figure 3a may be used, in which the interphase resistance is located totally within the solid pathway.

Then

$$\frac{1}{R_{tot}} = \frac{1}{R_f} + \frac{1}{R_s + R_{fs}} \tag{17}$$

$$= \frac{1}{R_{cf} + R_{wf}} + \frac{1}{R_{cs} + R_{fs} + R_{ws}} \tag{18}$$

Substituting in 17 gives

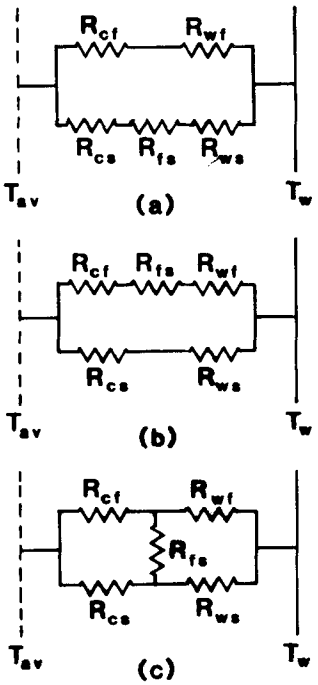

Figure 3. Alternative placements of the interphase resistance.

$$\frac{4\bar{k}_r}{R} = \frac{4\bar{k}_{rf}}{R} + \left[\frac{R}{4\bar{k}_{rs}} + \frac{2}{haR}\right]^{-1} \tag{19}$$

and multiplying by $R/4k_f$ and expanding the average conductivities ($k_r/\bar{k}_r = (Bi + 4)/Bi$, etc.) then

$$\frac{k_r}{k_f}\frac{Bi}{Bi + 4} = \frac{k_{rf}}{k_f}\frac{Bi_f}{Bi_f + 4} + \left[\frac{k_f}{k_{rs}}\frac{Bi_s + 4}{Bi_s} + \frac{8k_f}{haR^2}\right]^{-1} \tag{20}$$

Now defining $N_s \equiv haR^2/k_{rs}$ gives, upon rearrangement

$$\frac{k_r}{k_f}\frac{Bi}{Bi + 4} = \frac{k_{rf}}{k_f}\frac{Bi_f}{Bi_f + 4} + \frac{k_{rs}}{k_f}\left[\frac{8}{N_s} + \frac{Bi_s + 4}{Bi_s}\right]^{-1} \tag{21}$$

This expression does not allow the separation of k_r/k_f and Bi, and a second relationship must be found.

Assuming that at high flow rates the bed as a whole behaves in a similar fashion to the fluid phase, take

$$\frac{R_c}{R_w} = \frac{R_{cf}}{R_{wf}}$$

or

$$\frac{R}{4k_r}h_w = \frac{R}{4k_{rf}}h_{wf} \text{ so } Bi = Bi_f \tag{22}$$

Then multiplying through in the previous expression gives

$$\frac{k_r}{k_f} = \frac{k_{rf}}{k_f} + \frac{k_{rs}}{k_f}\frac{(Bi_f + 4)}{Bi_f}\left[\frac{8}{N_s} + \frac{Bi_s + 4}{Bi_s}\right]^{-1} \tag{23}$$

Equations 22 and 23 were derived before by a perturbation-collocation argument by Dixon and Cresswell (1979) and used successfully to predict k_r and Bi at moderate to high Re.

If the interphase resistance is omitted, Eq. 23 reduces to

$$\frac{k_r}{k_f} = \frac{k_{rf}}{k_f} + \frac{k_{rs}}{k_f}\left(\frac{Bi_s}{Bi_s + 4}\right)\left(\frac{Bi_f + 4}{Bi_f}\right) \tag{24}$$

and on recognizing that

$$\frac{k_{rs}}{k_f} = \left(1 + \frac{4}{Bi_s}\right)\frac{\bar{k}_{rs}}{k_f}$$

the "short form" of Melanson and Dixon (1985) is obtained

$$\frac{k_r}{k_f} = \frac{k_{rf}}{k_f} + \frac{\bar{k}_{rs}}{k_f}\frac{Bi_f + 4}{Bi_f} \tag{25}$$

which they showed differs insignificantly from the longer form of Eq. 23 for steady state modeling at reasonable flow rates.

By analogy with mass transfer studies (Dixon et al., 1984) it is known that for large Re, k_{rf} is proportional to Re, whereas Bi_f is proportional to $Re^{-0.4}$, so that $(Bi_f + 4)/Bi_f \propto Re^{0.4}$; thus the fluid contribution does dominate Eq. 25 for $Re \to \infty$; however, the solid contribution is significant, certainly over the Re range usual in laboratory work.

It would not be correct to examine the limit $Re \to 0$ under the current high Re case; however, it may be noted that Eq. 24 may also be written as

$$\frac{1}{Pe_r} = \frac{1}{Pe_{rf}} + \frac{k_{rs}/k_f}{RePr}\left(\frac{Bi_s}{Bi_s + 4}\right)\left(\frac{Bi_f + 4}{Bi_f}\right) \tag{26}$$

and that as $Re \to 0$, $Pe_r \to 0$ also, regardless of the behavior of Bi_f. Thus values of Pe_r may be relatively accurately predicted by this formula even for low Re, although the derivation of it is inapplicable to that case.

Low *Re* Case

At low enough flow rates conduction becomes the dominant transport mechanism, and most of the energy is transferred directly through the solid phase. The simplified picture of Figure 3b may be applied, and the development is analogous to the high Re case:

$$\frac{1}{R_{\text{tot}}} = \frac{1}{R_f + R_{fs}} + \frac{1}{R_s} \tag{27}$$

$$= \frac{1}{R_{cf} + R_{fs} + R_{wf}} + \frac{1}{R_{cs} + R_{ws}} \tag{28}$$

leading to

$$\frac{k_r}{k_f}\left(\frac{Bi}{Bi + 4}\right) = \frac{k_{rs}}{k_f}\left(\frac{Bi_s}{Bi_s + 4}\right) + \frac{k_{rf}}{k_f}\left[\frac{Bi_f + 4}{Bi_f} + \frac{8}{N_F}\right]^{-1} \tag{29}$$

using the definition

$$N_F = \frac{haR^2}{k_{rf}}$$

This time set

$$\frac{R_c}{R_w} = \frac{R_{cs}}{R_{ws}} \tag{30}$$

giving $Bi = Bi_s$ and also

$$\frac{k_r}{k_f} = \frac{k_{rs}}{k_f} + \frac{k_{rf}}{k_f}\frac{(Bi_s + 4)}{Bi_s}\left[\frac{Bi_f + 4}{Bi_f} + \frac{8}{N_F}\right]^{-1} \tag{31}$$

Again omitting the interphase resistance leads to a short form

$$\frac{k_r}{k_f} = \frac{k_{rs}}{k_f} + \frac{k_{rf}}{k_f}\left(\frac{Bi_s + 4}{Bi_s}\right)\left(\frac{Bi_f}{Bi_f + 4}\right) \tag{32}$$

This case may be correctly reduced to the limit $Re \to 0$, giving

$$\frac{k_r^\circ}{k_f} = \frac{k_{rs}}{k_f} + \epsilon\left(1 + \frac{h_{rv}d_p}{k_f}\right)\left(\frac{Bi_s + 4}{Bi_s}\right)\left(\frac{Bi_f^\circ}{Bi_f^\circ + 4}\right) \tag{33}$$

where Bi_f° is the limiting value of Bi_f as $Re \to 0$. This value has not yet been established by fluid phase studies, although Eq. 33 suggests that it should be nonzero to retain the fluid contribution to k_r°.

Equation 33 also shows that the fluid phase contribution to the stagnant conductivity should be corrected for wall effects, at least for low d_t/d_p. In laboratory experiments this term is usually negligibly small in comparison with k_{rs}, so that the relative success of stagnant conductivity prediction formulas that omit this correction (for example, Kunii and Smith, 1960) is not surprising. At higher temperatures, where radiation is significant, the correction may be important.

The inappropriate limit of $Re \to \infty$, applied to Eq. 32, gives $k_r \propto Re^{0.6}$, which is not observed experimentally, and hence this equation will not do for the entire range of Re.

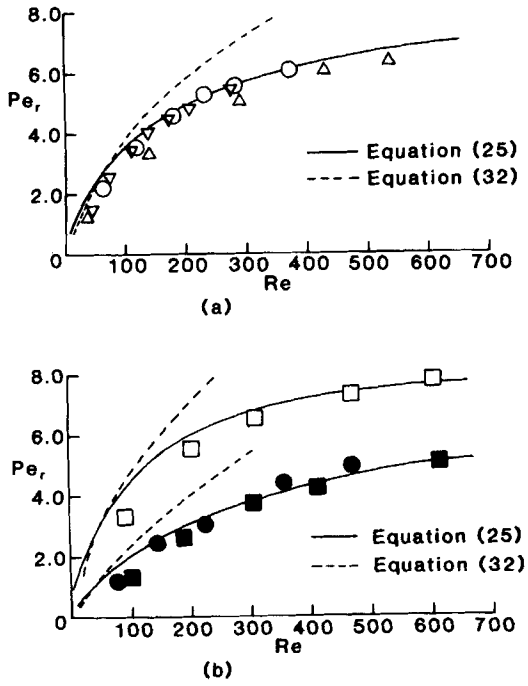

Figure 4. Comparison of formulas with data for Pe_r.

Intermediate *Re* Case

For the case when significant energy is transferred through both phases, one might try a resistance network such as that shown in Figure 3c. The difficulties arising from placing R_{fs} between the phases are demonstrated by solving even this very simple network, which, after some gruelling algebra, finally yields

$$\frac{k_r}{k_f}\frac{Bi}{Bi+4}=\frac{\dfrac{k_{rs}}{k_f}\dfrac{Bi_s}{Bi_s+4}+\dfrac{k_{rf}}{k_f}\dfrac{Bi_f}{Bi_f+4}+\dfrac{1}{2}\left(\dfrac{Bi_f}{Bi_f+4}\dfrac{Bi_s}{Bi_s+4}\right)\left(\dfrac{k_{rf}}{k_f}+\dfrac{k_{rs}}{k_f}\right)\left(\dfrac{N_s}{Bi_s}+\dfrac{N_F}{Bi_f}\right)}{1+\dfrac{1}{2}\left(\dfrac{N_s}{Bi_s+4}+\dfrac{N_F}{Bi_f+4}\right)} \tag{34}$$

This result acts as a strong incentive to develop simpler approaches, and it is expedient to let $N_s, N_F \to 0$ above, which gives

$$\frac{k_r}{k_f}\frac{Bi}{Bi+4}=\frac{k_{rs}}{k_f}\frac{Bi_s}{Bi_s+4}+\frac{k_{rf}}{k_f}\frac{Bi_f}{Bi_f+4} \tag{35}$$

and corresponds once more to the omission of interphase resistance.

As *Re* decreases, the sublayer of stagnant fluid next to the wall grows thicker, and most of the energy is transferred by damped turbulent mixing up to this sublayer, followed by interphase transfer and conduction through the thinner solid phase fillets. So

$$\frac{1}{Bi}\simeq\frac{1}{Bi_f}+\frac{1}{Bi_s} \tag{36}$$

which follows from a picture of fluid and solid resistances in series; and then

$$\frac{k_r}{k_f}=\left(1+4\frac{Bi_f+Bi_s}{Bi_fBi_s}\right)\left\{\frac{k_{rs}}{k_f}\frac{Bi_s}{Bi_s+4}+\frac{k_{rf}}{k_f}\frac{Bi_f}{Bi_f+4}\right\} \tag{37}$$

These equations reduce to Eqs. 22 and 24, as $Re \to \infty$, and to Eqs. 30 and 32, as $Re \to 0$.

COMPARISON OF FORMULAS WITH DATA

The problem of finding adequate experimental data to test the model-matching theory was discussed by Dixon and Cresswell (1979) and involved questions of the correct selection of experimental conditions, the choice of a statistically adequate model for analysis of the data, and the use of unbiased parameter estimation methods. In addition, the comparisons of Eqs. 22 and 23 with data from several sources made in that earlier work were adversely affected by both the unavailability of suitable correlations for the single-phase parameters and the lack of complete information on voidage, particle conductivity, and sometimes even an unambiguous flow rate for some of the studies.

The comparisons here are made mainly with data for the intermediate *Re* range, namely, the results of Dixon et al. (1978) for ceramic and steel spheres, supplemented with unpublished data available from further experiments made in conjunction with this study. The equipment used for these new experiments was a facsimile of that for the earlier work and has been adequately described there (Dixon et al., 1978). The packings used were nylon and steel spheres, and the method of data analysis was also identical to that of the previous work. The comparisons are limited to data taken for spherical packings, as the fluid mixing contribution k_{rf} has not been adequately investigated for nonspherical particles. Further, it should be noted that for *Bi* a separate comparison must be made for each d_t/d_p value, so literature data have been selected to give similar d_t/d_p ratios to those of Dixon et al. (1978) and the present study.

The single-phase parameters were obtained from the correlations of Dixon et al. (1984) for the fluid phase and of Melanson and Dixon (1985) for the solid phase. Details on the packing materials are also available in those references.

Figure 4 shows the comparison between data and the limiting case short forms, Eqs. 25 and 32, for the radial Peclet number. Ceramic spheres (average $d_t/d_p = 7.6$) are shown in Figure 4a, nylon and steel spheres in Figure 4b. As expected, the high *Re* formula is close to the data for the entire *Re* range, while the low *Re* formula deviates seriously as *Re* increases. There is a transition point at which Eq. 32 is better than Eq. 25, but this is at very low *Re* and is barely supported by the data. The intermediate Eq. 37 is not shown, but underpredicts Pe_r consistently, coming close to the data for high and low *Re* only. In view of the good agreement of Eq. 25, an intermediate formula is not considered necessary for Pe_r.

In Figure 4a, the packings are all of the same thermal conductivity, with $5.6 \leq d_t/d_p \leq 11.1$. The dependence of Pe_r on d_t/d_p is clearly weak, which should not be surprising as k_r should represent bed-center phenomena more than wall effects. An average d_t/d_p of 7.6 was used in the predictive formulas in Figure 4a; predicted values are also relatively insensitive to d_t/d_p. Figure 4b shows packings of the same d_t/d_p but very different particle conductivity (nylon vs. steel). The strong dependence of Pe_r on k_{rs} is quite clear, and over the *Re* range considered, the effective conductivity appears to be accounted for equally by fluid mixing and wall-corrected solid conduction.

The comparison between predicted and experimental *Bi* is made in Figures 5 to 8, where the transition of the data between high *Re* and low *Re* asymptotes is clearly seen. The intermediate Eq. 36 agrees well with the qualitative trends of the data but underpredicts all except the 6.4 mm ceramic spheres results. In general the data lie within the envelope bounded by Eqs. 22, 30, and 36.

A comparison of Figures 5 and 6 shows that *Bi* is relatively independent of particle conductivity in the intermediate to high *Re* range. However, Figures 7 and 8 show that there is a reasonable dependence on d_t/d_p, especially for low intermediate *Re*. Figure 7 shows the lowest d_t/d_p value, and the results of Kunii et al. (1968), which were obtained in the range $300 < Re < 8000$, have been used to extend the data base to high *Re*. These results show good agreement with the high *Re* asymptote of $Bi = Bi_f \propto Re^{-0.4}$ and also give some indication of the uncertainty in estimates of *Bi*, in conjunction with the data of Dixon et al. (1978). Figure 8 shows

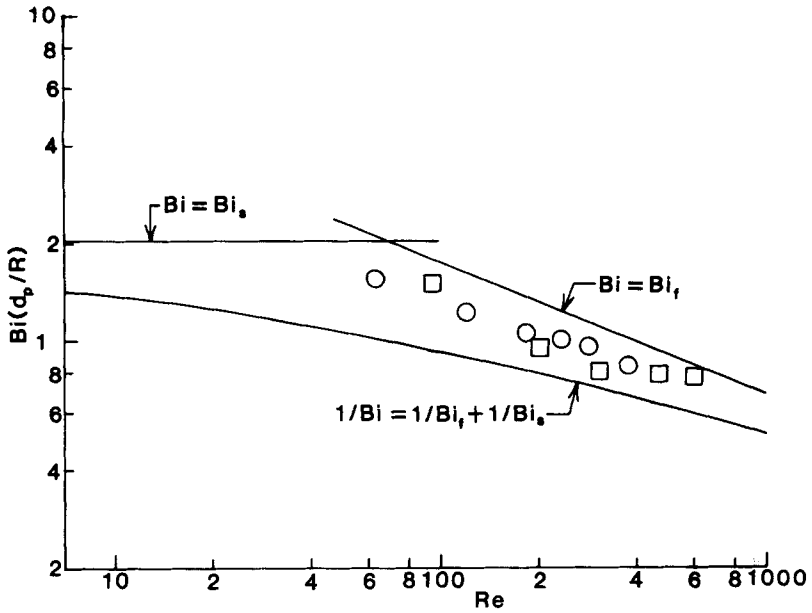

Figure 5. Comparison of formulas for *Bi* with data for 9.5 mm ceramic spheres and nylon spheres (d_t/d_p = 7.6).

higher d_t/d_p data, supplemented at lower Re by the results of Valstar et al. (1975). The data in Figure 8 lie closer to the intermediate Re formula, Eq. 36, than in the other cases. The fluid phase radial Peclet number Pe_{rf}, used in the calculation of Bi_f, was, however, taken as $Pe_{rf} = 10$ throughout. There is some evidence (Dixon et al., 1984) to suggest that a value of 8 may be more appropriate as d_t/d_p increases, which would lower the predictions. The formulas would then bracket the data as in Figures 5–7.

This analysis does much to explain previous empirical results. The Biot number asymptotes give $Bi_s \propto Re^{0.0}$ and $Bi_f \propto Re^{-0.4}$; now data taken under laboratory conditions almost always fall into the transition region, so that the exponent on Re should be between these limits. Indeed, Dixon et al. (1978) fitted the empirical expression

$$Bi = 5.73\sqrt{\frac{d_t}{d_p}}\,Re^{-0.262} \tag{38}$$

to the data shown here. Furthermore, the wall heat transfer coefficient was frequently correlated directly against Re in early fixed-bed heat transfer studies, and the wide range of exponents found has been remarked upon by Beek (1962) and Froment and Bischoff (1979), among others. Now $Bi = h_w R/k_r$ and $k_r \propto Re$, so that it should be expected that $h_w \propto Re^{\alpha}$, where $0.6 < \alpha < 1.0$; indeed, most of the studies quoted by Beek (1962) gave exponents in that range. The particular value of α would depend in which part of the transition region the data were taken. Later studies have favored the use of the Nusselt number $Nu_w (= h_w d_p/k_f)$ as a dimensionless form. The wide scatter in empirical correlations for this parameter was partially explained by Dixon and Cresswell (1979), and it is now seen that the transition region is responsible in large part for the apparent disagreement between various studies.

COMPARISON WITH PREVIOUS MODELS

Several workers (Yagi and Kunii, 1957; DeWasch and Froment, 1972; Bauer and Schlünder, 1978) have used a simple addition

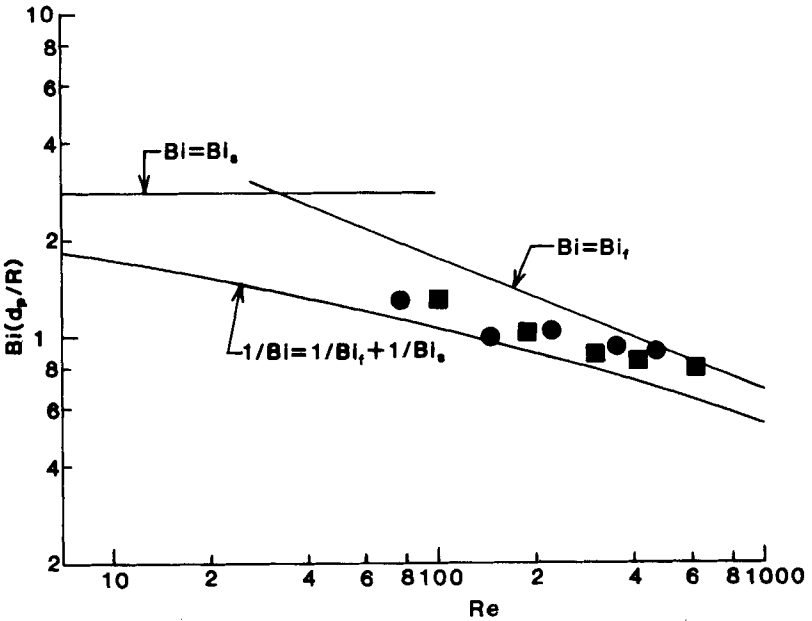

Figure 6. Comparison of formulas for *Bi* with data for 9.5 mm steel spheres (d_t/d_p = 7.6).

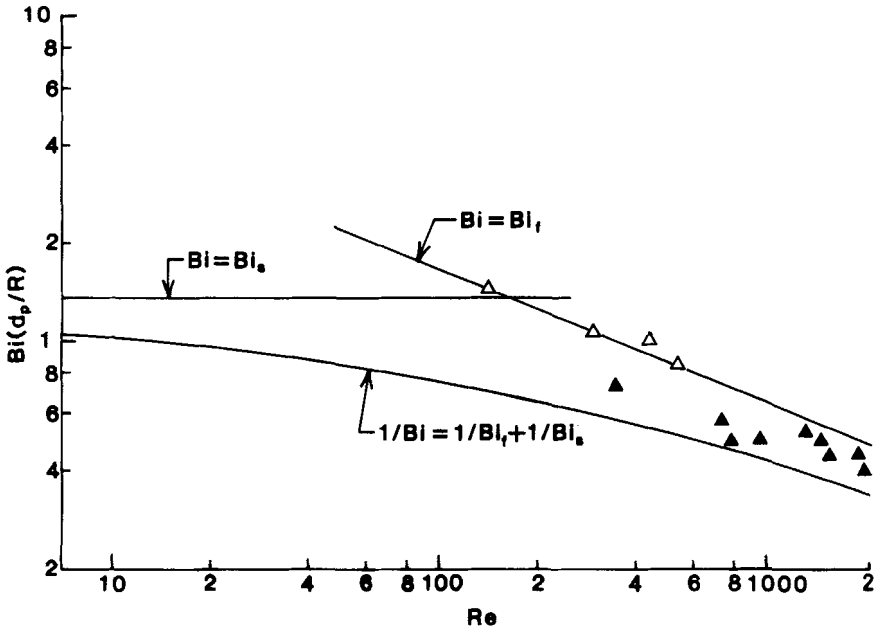

Figure 7. Comparison of formulas for *Bi* with data for 12.7 mm ceramic spheres (d_t/d_p = 5.6) and 28.0 mm cellite spheres (d_t/d_p = 5.0).

formula for both effective parameters:

$$k_r = k_{rs} + k_{rf} \tag{39}$$

and

$$h_w = h_{ws} + h_{wf} \tag{40}$$

Looking at the implications of this in terms of resistances, the equivalent formulas are

$$\begin{aligned} &\text{i)}\ \frac{1}{R_c} = \frac{1}{R_{cs}} + \frac{1}{R_{cf}} \\ &\text{ii)}\ \frac{1}{R_w} = \frac{1}{R_{ws}} + \frac{1}{R_{wf}} \\ &\text{iii)}\ R_{\text{tot}} = R_c + R_w \end{aligned} \tag{41}$$

The resistance network corresponding to this is shown in Figure 9a; it should be noted that a decomposition of resistance by region is implied by the use of Eqs. 41(i) and 41(ii), followed by a decomposition by phase.

The inadequacies of Eq. 39 in predicting k_r for beds in which wall effects are important have been demonstrated by Dixon and Cresswell (1979). The use of Eq. 40 has not been tested to such an extent. Perhaps the most complete development of a prediction formula for h_w is that of Kunii and coworkers (Kunii and Suzuki, 1966, 1969; Kunii et al., 1968); their modification of the resistance network is shown in Figures 9b and 9c.

The main distinctive feature of their work is the assumption that wall effects are restricted to a region of thickness $d_p/2$ next to the wall. They preferred to define an effective conductivity for the wall region, rather than the heat transfer coefficient h_w, which they computed from

$$\frac{1}{h_w} = \frac{d_p/2}{k_{rw}} - \frac{d_p/2}{k_r} \tag{42}$$

rather than predicting directly. The resistance network of Figure 9c leads to

$$\frac{1}{R_w} = \frac{1}{R_{ws}} + \frac{1}{R_{wf} + R^*_{wf}} \tag{43}$$

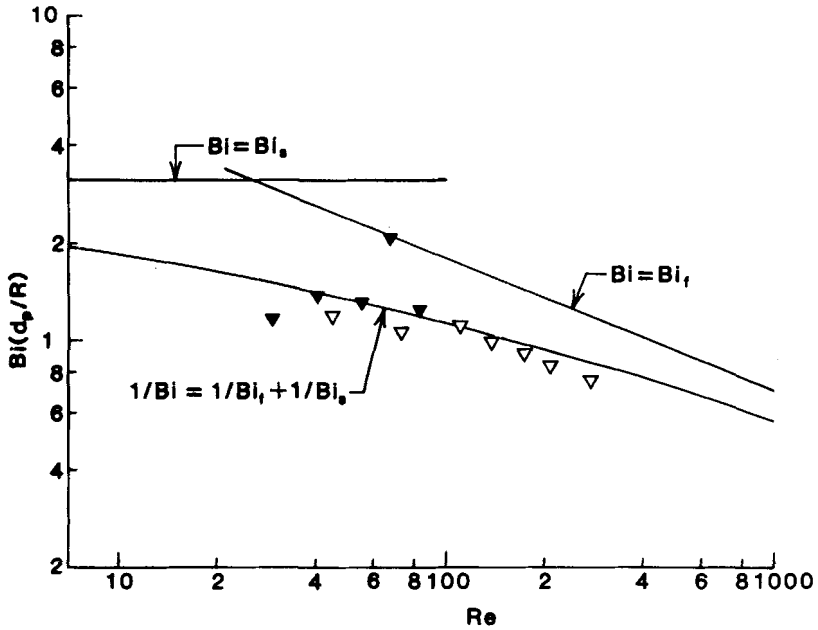

Figure 8. Comparison of formulas for *Bi* with data for 6.4 mm ceramic spheres (d_t/d_p = 11.1) and 3.7 mm glass spheres (d_t/d_p = 11.1).

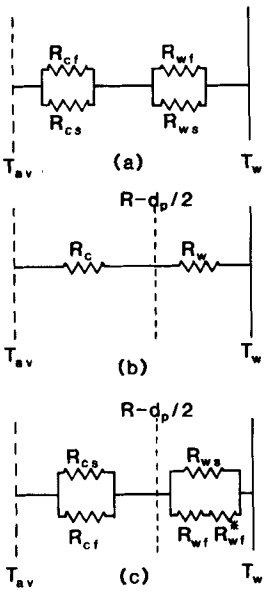

Figure 9. Resistance models for previous work.

and thence

$$k_{rw} = k^\circ_{rw} + \frac{1}{\dfrac{1}{k_{wf}} + \dfrac{1}{h^*_w d_p/2}} \tag{44}$$

The k°_{rw} was obtained from a modification of the Kunii-Smith (1960) formula for stagnant conductivity. A random walk analysis of fluid mixing in the near-wall region gave (Kunii and Suzuki, 1966)

$$\frac{k_{wf}}{k_f} = 0.02\, RePr \tag{45}$$

and h^*_w was obtained empirically by analogy with mass transfer experiments (Kunii and Suzuki, 1969). The effective conductivity k_r was obtained from Eq. 39 in the form suggested by Yagi and Kunii (1957):

$$\frac{k_r}{k_f} = \frac{k^\circ_r}{k_f} + 0.10\, PrRe \tag{46}$$

The results of Eqs. 42–46 are here evaluated for steel spheres ($d_t/d_p = 7.5$) in Table 1; trends for ceramic spheres were similar. As expected, Eq. 46 underpredicts k_r, even taking the highest reasonable value of k°_r. The Bi values were computed using k_r from both Eqs. 46 and 25 and in both cases fall below the experimental values shown in Figure 6.

The basic problem with this approach is the arbitrary choice of $d_p/2$ as the width of the near-wall region. Decomposition by region makes sense when the wall effects really are confined to a layer near the wall, as is the case for large d_t/d_p beds. Comparisons with data from such beds have been largely successful. For beds with $d_t/d_p < 10$, however, the entire bed is affected by the walls, and no true center region exists. In this case, the approach of decomposing resistance *first by phase* corresponds more nearly to reality, and this has been illustrated by the success of the formulas derived in this way. As d_t/d_p increases, the differences between the two points of view become less and are unimportant for $d_t/d_p > 15$–20.

An interesting parallel may be drawn with the work of Crane and Vachon (1977) on effective conductivity of granular materials under stagnant conditions. The thermal resistance analyses are referred to as Ohm's law models in their paper, and they distinguish two ways of obtaining resistance networks. The network shown in Figure 2d corresponds to an assumption of zero lateral conductivity, or uniform heat flow in the direction of the overall temperature gradient, in this case the radial direction. As the resistance of the individual parallel branches (fluid and solid) differ, the potential (temperature) will be different in each lateral plane. Conversely,

TABLE 1. PREDICTIONS OF THE FORMULAS OF KUNII ET AL. FOR STEEL SPHERES, $d_t/d_p = 7.5$

			Eq. 46		Eq. 25	
Re	h^*_w	k_{rw}	k_r	$Bi\left(\frac{d_p}{R}\right)$	k_r	$Bi\left(\frac{d_p}{R}\right)$
100	21.5	0.23	0.76	0.87	1.08	0.54
200	36.1	0.26	0.97	0.73	1.39	0.46
300	49.0	0.28	1.19	0.62	1.68	0.40
400	60.8	0.31	1.40	0.57	1.96	0.38
500	71.8	0.33	1.62	0.51	2.23	0.35

the network shown in Figure 9a corresponds to an assumption of infinite lateral conductivity, so that the potential is constant in each lateral plane, and the radial heat flow along each branch is not constant. Thus, at a distance of $d_p/2$ (or any other) from the wall, the fluid and solid temperatures can be taken as equal, allowing the two branches to meet. Crane and Vachon found that the two approaches produced bounds on a wide range of experimental data, which narrowed as the ratio of phase conductivities became closer to unity. In the present case this ratio is k_{rs}/k_{rf}, which should certainly depart from unity as Re increases. It is quite consistent, therefore, that there are considerable differences in the predictions of equations based on the different thermal resistance models.

The persistent discrepancies in the predictions of Eqs. 42–46 are due, as remarked above, to the need to choose a point at which to change from center-bed resistances to wall-region resistances. Such a point is invariably chosen close to the wall, where it is unlikely that fluid and solid temperatures are really equal, as is assumed in 42–46. The identity of the two approaches in the limit $d_t/d_p \to \infty$ is due to the extra resistance in the wall region becoming negligible compared to the center-bed resistance.

Finally it may be noted that the intuitively appealing idea of additivity of the fluid and solid phase conductivities, due to their mechanisms acting in parallel, has not been altogether lost. Instead, Eq. 14 shows that it must be applied to total, or bed average, conductivities only, and not to those in subregions of the bed.

THERMAL RESISTANCE MODELS OF AXIAL HEAT TRANSFER

The perturbation-collocation analysis of Dixon and Cresswell (1979) led to the formula

$$k_a = k_{af} + k_{as}\left[1 + \frac{2}{haR}\frac{4k_{rs}}{R}\frac{Bi_s}{Bi_s + 4}\right]^2 \tag{47}$$

for the effective axial conductivity. This may also be interpreted in terms of resistances, and with obvious changes in notation, gives

$$\frac{1}{R_{a,\text{tot}}} = \frac{1}{R_{af}} + \frac{1}{R_{as}}\left[\frac{R_s}{R_s + R_{fs}}\right]^2 \tag{48}$$

It does not appear possible, however, to find any physical model that is represented by this combination of resistances. It may be noted, however, that if interphase resistance is ignored ($R_{fs} = 0$), then a simple addition of resistances in parallel results

$$\frac{1}{R_{a,\text{tot}}} = \frac{1}{R_{af}} + \frac{1}{R_{as}} \tag{49}$$

In fact numerical evaluation of the bracketed term above shows that it is close to unity for all but small values of Re.

The above observations, in addition to the somewhat arbitrary placement of R_{fs} for the radial heat transfer case, suggest that the appearance of the interphase terms in the model matching formulas may well be an artifact of the particular approximation method chosen. The radial discretization of the two-phase model equations leads to a coupled pair of boundary-value problems, which may be solved analytically only in two special cases:

1. Equality of solid and fluid temperatures.

2. Negligible axial conduction in the solid phase.

Dixon and Cresswell (1979) developed an approximate solution by perturbation away from the exact solution found under the second assumption above. It is thus not surprising that the axial effective conductivity formula was affected by that choice.

It is also possible to develop an approximate solution by perturbing away from the exact solution found under the first assumption above, by identifying N_s as a large parameter in the equation, rather than k_{as} as a small one. The model-matching formulas obtained in that case are

$$k_a = k_{af} + k_{as} \tag{50}$$

and

$$\frac{k_r}{k_f}\frac{Bi}{Bi+4} = \frac{k_{rf}}{k_f}\frac{Bi_f}{Bi_f+4} + \frac{k_{rs}}{k_f}\frac{Bi_s}{Bi_s+4} \tag{35}$$

and the interphase terms do not appear.

It can be shown that identifying N_s as a large parameter is equivalent to assuming large Re; a similar analysis can be made for small Re. Both collocation-perturbation analyses give Eqs. 35 and 50. For high Re it is then appropriate to match the one-phase and fluid temperatures, giving $Bi = Bi_f$, and for low Re one matches one-phase and solid temperatures, giving $Bi = Bi_s$; the earlier "short form" results then follow directly.

NOTATION

All heat transfer parameters defined in terms of total area (void + nonvoid) normal to the direction of heat transfer.

a = specific interfacial surface area
d_p = pellet diameter
d_t = tube diameter
G = superficial mass flow rate
h = heat transfer coefficient
h^* = wall thermal layer heat transfer coefficient
h_{rv} = fluid radiation heat transfer coefficient
k = thermal conductivity
$\bar{k}$ = bed average thermal conductivity
k° = stagnant bed thermal conductivity
q_r = radial heat flux
r = radial coordinate
R = tube radius (when unsubscripted)
R = thermal resistance per unit wall area (subscripted)
T_{av} = bed average temperature
T_c = bed centerline temperature
T_w = temperature of heated section wall
U = overall heat transfer coefficient (based on $T_w - T_{av}$)
U' = overall heat transfer coefficient (based on $T_w - T_c$)
Bi = wall Biot number ($h_w R/k_r$)
Bi° = stagnant bed wall Biot number ($h_w^\circ R/k_r^\circ$)
N_s = ahR^2/k_{rs}
N_F = ahR^2/k_{rf}
Nu = Nusselt number (hd_p/k_f)
Pe = heat transfer Peclet number ($Gc_f d_p/k$)
Pr = Prandtl number ($\mu c_f/k_f$)
Re = Reynolds number (Gd_p/μ)

Greek Letters

ϵ = bed void fraction
λ_1 = smallest root of $BiJ_o(\lambda) - \lambda J_1(\lambda) = 0$

Subscripts

a = axial
c = centerbed
f = fluid phase
p = pellet
r = radial
s = solid phase
w = wall

LITERATURE CITED

Bauer, R., and E. U. Schlünder, "Effective Radial Thermal Conductivity of Packings in Gas Flow. I. Convective Transport Coefficient," *Int. Chem. Eng.*, **18**, 181 (1978).

Beek, J., "Design of Packed Catalytic Reactors," *Adv. Chem. Eng.*, **3**, 203 (1962).

Beek, J., and E. Singer, "A Procedure for Scaling-up a Catalytic Reactor," *Chem. Eng. Progr.*, **47**, 534 (1951).

Crane, R. A., and R. I. Vachon, "A Prediction of the Bounds on the Effective Thermal Conductivity of Granular Materials," *Int. J. Heat Mass Transfer*, **20**, 711 (1977).

Cresswell, D. L., and A. G. Dixon, "Reply to Comments by Vortmeyer and Berninger on the Paper "Theoretical Prediction of Effective Heat Transfer Parameters in Packed Beds (AIChE J. 25, 663, 1979)," " *AIChE J.*, **28**, 511 (1982).

Crider, J. E., and A. S. Foss, "Effective Wall Heat Transfer Coefficients and Thermal Resistances in Mathematical Models of Packed Beds," *AIChE J.*, **11**, 1012 (1965).

DeWasch, A. P., and G. F. Froment, "Heat Transfer in Packed Beds," *Chem. Eng. Sci.*, **27**, 567 (1972).

Dixon, A. G., and D. L. Cresswell, "Theoretical Prediction of Effective Heat Transfer Parameters in Packed Beds," *AIChE J.*, **25**, 663 (1979).

Dixon, A. G., D. L. Cresswell, and W. R. Paterson, "Heat Transfer in Packed Beds of Low Tube/Particle Diameter Ratio," *ACS Symp. Ser. No. 65*, 238 (1978).

Dixon, A. G., M. A. DiCostanzo and B. A. Soucy, "Fluid Phase Radial Transport in Packed Beds of Low Tube-to-Particle Diameter Ratio," *Int. J. Heat Mass Transfer*, **27**, 1701 (1984).

Finlayson, B. A., "Packed Bed Reactor Analysis by Orthogonal Collocation," *Chem. Eng. Sci.*, **26**, 1081 (1971).

Froment, G. F., "Fixed Bed Reactors. Steady State Conditions," *Proc. 2nd ISCRE*, Elsevier, Amsterdam (1972).

Froment, G. F., and K. B. Bischoff, *Chemical Reactor Analysis and Design*, Wiley, New York (1979).

Hlavacek, V., "Aspects in Design of Packed Catalytic Reactors," *Ind. Eng. Chem.*, **62**, 9 (1970).

Kunii, D., and J. M. Smith, "Heat Transfer Characteristics of Porous Rocks," *AIChE J.*, **6**, 71 (1960).

Kunii, D., and M. Suzuki, "Heat Transfer Between Wall Surface and Packed Solids," *Int. Heat Transfer Conf.* (Chicago) IV, 334 (1966).

———, "Heat and Mass Transfer from Wall Surface to Packed Beds," *J. Fac. Eng. Univ. Tokyo (B)*, **30** (1969).

Kunii, D., M. Suzuki, and N. Ono, "Heat Transfer from Wall Surface to Packed Beds at High Reynolds Number," *J. Chem. Eng. Japan*, **1**, 21 (1968).

Melanson, M. M., and A. G. Dixon, "Solid Conduction in Low d_t/d_p Fixed Beds of Spheres, Pellets and Rings," *Int. J. Heat Mass Transfer*, **28**, 383 (1985).

Valstar, J. M., P. J. Van Den Berg, and J. Oyserman, "Comparison Between Two-dimensional Fixed Bed Reactor Calculations and Measurements," *Chem. Eng. Sci.*, **30**, 723 (1975).

Villadsen, J., and M. Michelsen, *Solution of Differential Equation Models by Polynomial Approximation*, Prentice-Hall, Englewood Cliffs, (1978).

Wellauer, T., D. L. Cresswell, and E. J. Newson, "Heat Transfer in Packed Reactor Tubes Suitable for Selective Oxidation," *ACS Symp. Ser. No. 196*, 527 (1982).

Yagi, S., and D. Kunii, "Studies on Effective Thermal Conductivities in Packed Beds," *AIChE J.*, **3**, 373 (1957).

Manuscript received Feb. 14, 1984; revision received June 19, 1984, and accepted July 2.